DYNAMIC UXO CLASSIFICATION SENSORS: ADVANCED DIGITAL GEOPHYSICAL MAPPING FOR MUNITIONS RESPONSE SITES

Jonathan S. Miller, Senior Engineer, White River Technologies
Gregory Schultz, Chief Technology Officer, White River Technologies
Fridon Shubitidze, Senior Scientist, White River Technologies
Joe Keranen, Research Scientist, White River Technologies

Corresponding Author:
Jonathan S. Miller
White River Technologies
115 Etna Rd., Building 3, Suite 1
Lebanon, New Hampshire 03766
email: miller@whitervertech.com

Abstract

Digital Geophysical Mapping (DGM) is a critical part of the remediation process for sites containing Munitions and Explosives of Concern (MEC). Specifically, implementing Electromagnetic Induction (EMI) sensor surveys at these sites is an effective method for identifying potential Unexploded Ordnance (UXO) or other MEC. Such contaminants often contain significant amounts of metal that produce electromagnetic anomalies in the DGM survey data. In recent years, a new class of advanced EMI sensors has demonstrated the additional capability to discriminate innocuous clutter from potentially hazardous UXO/MEC. These advanced sensors incorporate multi-axis transmitters and receivers to better characterize magnetic field anomaly sources, thus enabling not only detection of MEC contaminants, but also clutter discrimination as well as classification of specific MEC types. We have developed a next generation set of advanced EMI sensors, which combine the mapping capabilities of previous DGM survey instruments with the high-resolution discrimination and classification capabilities of advanced characterization arrays. Here we present results from recent field tests demonstrating the detection and classification capabilities of two advanced systems: one configured as a towed array and the other as a man-portable system. By enabling high-resolution mapping, as well as discrimination and classification of MEC, these systems provide a significant advancement in geophysical survey capabilities over those of current industry workhorse instruments, particularly for sites containing large quantities of non-hazardous clutter. By integrating the detection, clutter rejection, and UXO/MEC classification stages in one survey, these capability improvements are realized through a reduction in the number of excavations required for scrap/clutter, a reduction in the total survey time required for detection and classification, and superior Quality Control (QC) due to the use of a single sensor for detection and classification.

Keywords: Munitions and Explosives of Concern (MEC), Unexploded Ordnance (UXO), Electromagnetic Induction (EMI), Digital Geophysical Mapping (DGM).

Introduction

Over the past 5 years or so, a significantly improved EMI technology has emerged and demonstrated the ability to provide high spatial and temporal resolution data that can be used to effectively discriminate clutter from UXO/MEC. These systems, which were primarily developed under the auspices of the U.S. Department of Defense (DOD) Environmental Security Technology Certification Program (ESTCP) Munitions Response program, incorporate multi-axis transmitter and receiver configurations that greatly increase the information contained in the data compared to data from the previous generation of EMI systems. These advanced systems have enabled a new classification approach that utilizes physical models to accurately predict the magnetic field from subsurface objects in order to extract useful model parameters corresponding to physical properties of potential UXO. These classification features may then be used to distinguish clutter from MEC during subsequent analysis of the features. Because the vast majority of the mapped anomalies are due to innocuous items such as metal scrap, litter, or fragmentation and munitions debris that are free of explosives, the ability to classify clutter and targets has become an extremely valuable way to reduce the time and costs associated with unnecessary excavations of non-hazardous debris (Andrews and Nelson, 2011).

These new advanced EMI systems were intended to operate as part of a secondary "cued" survey developed as an add-on to the existing geophysical survey workflow for UXO cleanup projects. By relying on the older style DGM survey data (such as those acquired from a Geonics EM-61 sensor) for anomaly identification (i.e., target picking), advanced sensors could be implemented in cued mode to revisit the location of each anomaly within the survey area and acquire very high resolution data with minimal impact to the overall flow.

Numerous demonstrations of this cued survey approach have shown it to be extremely effective for discriminating clutter from MEC at both demonstration and production sites (Andrews and others, 2011); however, the requirement for conducting an additional time consuming survey reduces the efficiency of the remediation process. Furthermore, because a lower resolution DGM sensor is often used to cue the target locations for the advanced EMI survey, it is sometimes difficult to reconcile the two data sets. This disconnect can lead to sensor placement errors during the cued survey that result in sub-optimal characterization of the target space (Miller and others, 2013).

With the proven performance of advanced EMI sensors and the trend towards acceptance of these technologies in the production environment (see www.serdp-estcp.org/Featured-Initiatives/Munitions-Response-Initiatives), the possibility now exists for shifting the focus of classification technology development from improved performance to improved efficiency and feasibility. Specifically, the development of sensors that provide both detection and target classification from the DGM survey would significantly enhance the efficiency and reliability of the classification process. Removing the cued survey from this process eliminates the costs and time associated with mobilization and deployment of a second system. Additionally, using one high resolution DGM data set to perform both the target picking and target classification stages enables a direct correlation between the 2-D map features and the classification features associated with each anomaly. This correlation is particularly useful for sites that contain high anomaly densities, environments that can be particularly challenging for deployment of cued sensors. Combining detection and UXO classification stages in one DGM survey, it is possible to make efficient and reliable decisions that lead directly to a substantial reduction in the number of unnecessary digs performed during remediation.

Classification: How Do Advanced EMI Systems Classify UXO and Clutter?

Advanced EMI sensors that produce high spatial and temporal resolution data provide the basis for munitions classification. The data produced by these sensors enable the application of physical models to data fitting methods, which yield useful classification parameters corresponding to physical properties of the object. A key requirement for classification sensors is the ability to produce multi-directional magnetic field illumination of objects in the subsurface. This capability is often achieved by incorporating multiple transmitters in the design. By producing three approximately orthogonal magnetic field vectors below the array, the sensor energizes objects within this space along three unique axes (Figure 1). This illumination generates electrical eddy currents that are distributed over the object as a function of the object's physical properties including its size, shape, and shell thickness. These eddy currents produce a secondary magnetic field that is measured by the induction coil receivers in the sensor array.

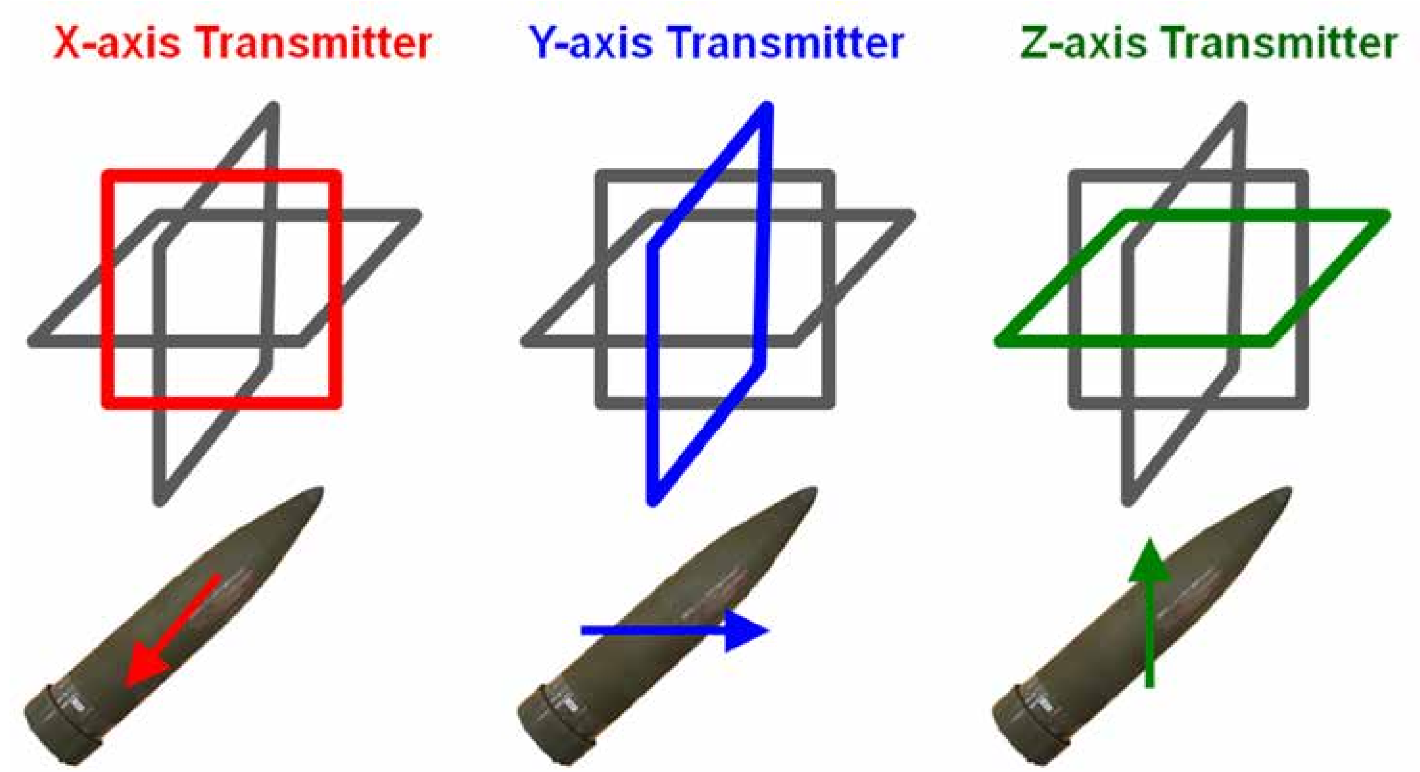

Figure 1: Advanced EMI sensors provide multi-axis illumination of an object by using multi-directional transmitters (TOP). Each transmitter produces a field that energizes a unique component of the object under interrogation (BOTTOM).

By energizing the object along three unique axes, the sensor produces eddy currents within the object that generate secondary fields similar to those produced by a set of equivalent magnetic dipoles oriented along the three principal axes of the object. The secondary fields measured by the sensor's receivers decay as a function of these three principal electromagnetic polarizabilities, which describe the object's electromagnetic response along each principal axis to the transmitter fields. As long as the transmitter fields are approximately orthogonal, these three principal polarizabilities will be well characterized by the data, regardless of the object's orientation or location relative to the sensor. In other words, the principal polarizabilities are intrinsic to each object and therefore produce effective and reliable classification features.

For an advanced EMI sensor data set, the principal polarizabilities may be extracted from the data using an iterative search method (i.e., geophysical inversion) to determine the model parameters that produce the closest match between the equivalent dipole model values and the observed data (e.g., Shubitidze and others, 2005; Bell and others, 2001). In this case, the objective function parameters include the object location parameters (e.g., x, y, z in Cartesian coordinates) and the three Euler rotation angles that determine the object's orientation. Once the objective function is minimized, the resulting dipole model polarizabilities can be used to classify an object as a target of interest (TOI) or clutter item (Figure 2). A TOI decision can be made by matching the extracted polarizabilities to those of known TOI libraries, or through feature based analysis using model parameters such as polarizability size and decay.

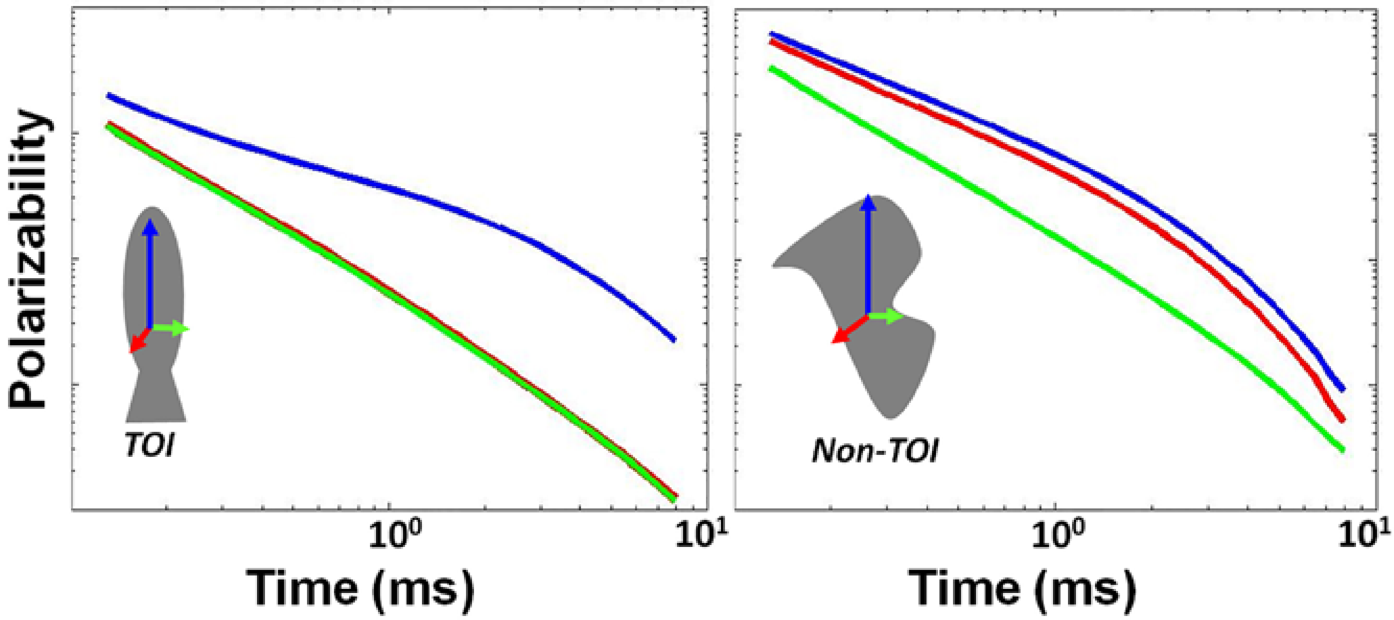

Figure 2: Primary (blue), secondary (red), and tertiary (green) polarizabilities associated with a TOI (LEFT) and a clutter item (RIGHT). The polarizabilities are associated with intrinsic object properties and can therefore be used to reliably make classification decisions. The symmetry of the TOI produces equivalent secondary and tertiary polarizabilities, whereas the asymmetry of clutter object produces three distinct polarizabilities. Polarizability units are arbitrary and are based on the output units of the sensor.

DGM Detection and Classification On-the-Move

The main challenge of performing effective classification using DGM survey data is to ensure all targets in the MRA are energized along three unique axes by the DGM sensor transmitter(s). With cued sensor classification, there is some a priori knowledge of target locations that is deduced from the DGM data analysis and can therefore guide the placement of the cued sensor. DGM sensors, however, are typically deployed along straight transects; thus, the sensor can encounter targets anywhere across its swath. Consequently, it is important that the DGM survey be designed to ensure effective multi-axis characterization for any target encountered in the swath covered while the sensor maintains an efficient survey pattern.

We developed a new DGM classification methodology that provides robust multi-axis characterization of targets in a DGM mode while mapping the survey area dynamically. We recently demonstrated two advanced DGM sensors at a DOD Standardized UXO Technology Demonstration Site. One system is a vehicle-towed sensor array designed for high production rates in open field areas; the other system is a smaller man portable array designed for operation in more challenging terrain. Our methodologies are tailored to the physical configurations of each sensor; however, both approaches produce effective clutter discrimination and UXO/MEC classification.

In the following sections, we provide a brief overview of how each of these systems works and we present some preliminary performance results from these recent field tests. These results clearly demonstrate the potential cost-savings of the combined detection/classification DGM approach that can be realized through an overall increase in survey efficiency, a reduction in the number of unnecessary digs, and an improvement in the reliability of the QC process.

Vehicle-Towed Array: Point Methodology

Our "OPTEMA" vehicle-towed array uses a configuration of five transmitter coils and 14 three-axis receiver coils spread across a 1.8m swath. The transmitter configuration comprises a large horizontal base transmitter (2m wide by 1m long) that encompasses four smaller (1m tall by 1m wide) vertical coils. The four vertical coils are connected in series pairs so that the transmitter array produces three effective coils (Figure 3).

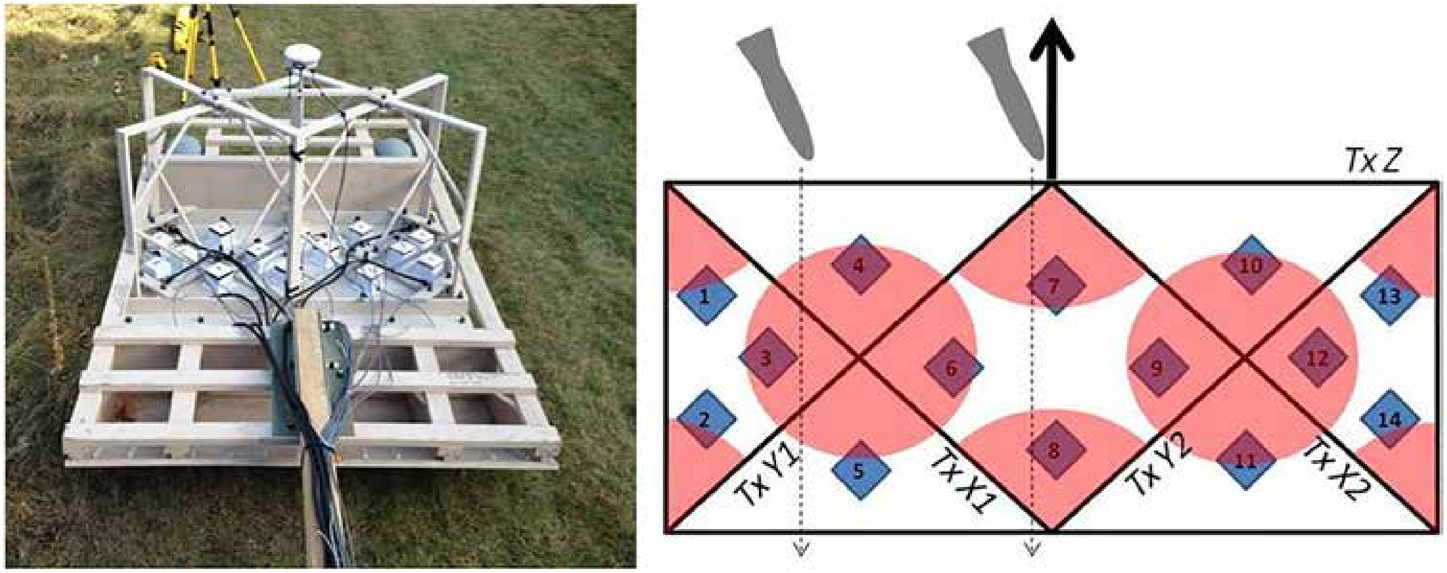

Figure 3: LEFT: Photograph of the OPTEMA sensor array tow platform. The multi-axis array is designed to provide good orthogonal magnetic field illumination across the entire sensor swath. The combination of full swath multi-axis illumination and high-spatial resolution sampling over the entire decay time period (0.1 to 8 ms) provides improved survey data over other advanced EMI systems that are limited in dynamic mode. RIGHT: Top-view of the transmitter and receiver layout. Regions that provide good orthogonal illumination are highlighted (red) around the transmitter coil (black lines) intersections. As the array passes over an object, the object will enter at least one of these regions regardless of its across track location. The resulting field scattered by the object is measured in one or more of the 14 three-axis receivers (blue diamonds).

This transmitter configuration ensures sufficient multi-axis illumination across the entire sensor swath. The orthogonality of the three transmitter fields is dependent to some extent on the depth of the target beneath the array; however, as a general guideline, the regions that contain the best multi-axis illumination from the transmitters are located below the intersections of three transmitter coils (Figure 3). Soundings acquired while the target passes through these regions provide data that fully constrain the inversion of all three principal axis polarizabilities and therefore each of these soundings enables classification of the target.

By treating each sounding (i.e., point location methodology) as a unique target encounter it is possible to obtain multiple sets of classification features for each DGM anomaly. The repeatability of various model parameters (e.g., target location, depth, orientation, polarizabilities, etc.) over multiple soundings associated with an anomaly may be used to build confidence in the classification decision. As an example, Figure 4 provides the set of model parameters associated with each sounding acquired in proximity to the anomaly circled in the DGM map. These parameters are consistent for each sounding, indicating the anomaly is well characterized.

One significant benefit of obtaining classification features from a single point location along each transect line is the reduced dependency on position and orientation data. Because there is no reliance in the inversion algorithm on point-to-point changes in the sensor array's position and orientation, it is possible to make effective classification decisions without high quality position and orientation data. This approach is particularly robust when high quality GPS and inertial data are not available or for instances when it may be difficult to track platform pitch and roll errors accurately.

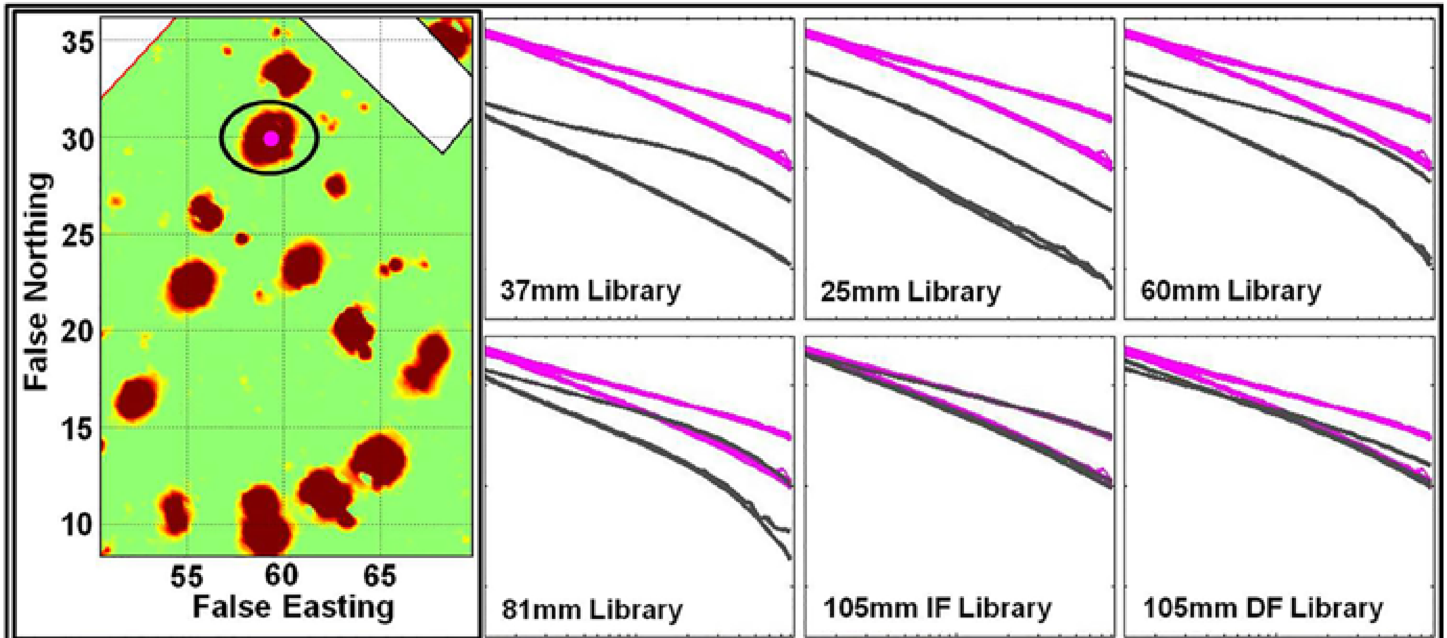

Sounding	Northing Error (m)	Easting Error (m)	Depth (m)	Azimuth (deg)	Dip (deg)
1	-0.003	0.026	-0.433	51.0	17.1
2	-0.009	0.027	-0.448	44.4	17.2
3	-0.003	0.000	-0.452	55.3	8.6
4	0.002	-0.001	-0.453	50.2	13.7
5	0.000	0.002	-0.455	40.7	10.5
6	-0.006	-0.002	-0.459	46.1	14.3
7	0.000	-0.008	-0.457	46.7	14.7
8	0.003	-0.017	-0.451	42.5	14.5
9	0.014	-0.029	-0.437	42.2	14.0

Figure 4: TOP LEFT: OPTEMA DGM Map (nanoTesla/sec) showing several anomalies (red blobs) in a portion of the MRA. The anomaly of interest is circled in black with the model-based estimated location shown as the magenta dot. TOP RIGHT: Library matching for six different UXO targets. These magnetic polarizability curves are plotted as a function of time (logarithmically spaced) from 0.1 to 8 ms. Polarizability units are arbitrary and correspond to the sensor output units. Soundings corresponding to the anomaly are selected for inversion and the resulting nine sets of polarizabilities (each set comprises a primary, secondary, and tertiary polarizability) are plotted in magenta against the TOI library polarizabilities (shown in dark grey). The polarizabilities obtained from these consecutive soundings are almost identical and show a clear match to the 105mm Indirect Fire munition type. BOTTOM: Estimated model parameters corresponding to each sounding. Parameters are highly consistent for each sounding, indicating a high confidence decision can be made. The Northing and Easting errors for each sounding are within +/- 3cm of the mean estimated location (shown as the magenta dot in the DGM map). Depth estimates are consistent to within +/- 2cm and orientation estimates are consistent within +/- 6 degrees.

Man-Portable Array: Line Methodology

Our "EMPACT" man-portable array features a compact 1.0m by 0.5m horizontal transmitter coil that encompasses 5 three-axis receiver coils. Because this sensor has only one transmitter coil, we aggregate the data from consecutive soundings along the transect line (i.e., line methodology) in order to ensure the target receives the required multi-axis illumination from the transmitter.

As the transmitter passes over the target, any offset of the sensor from directly over the target produces a different angle of incidence between the impinging transmitter field and the target (Figure 5).

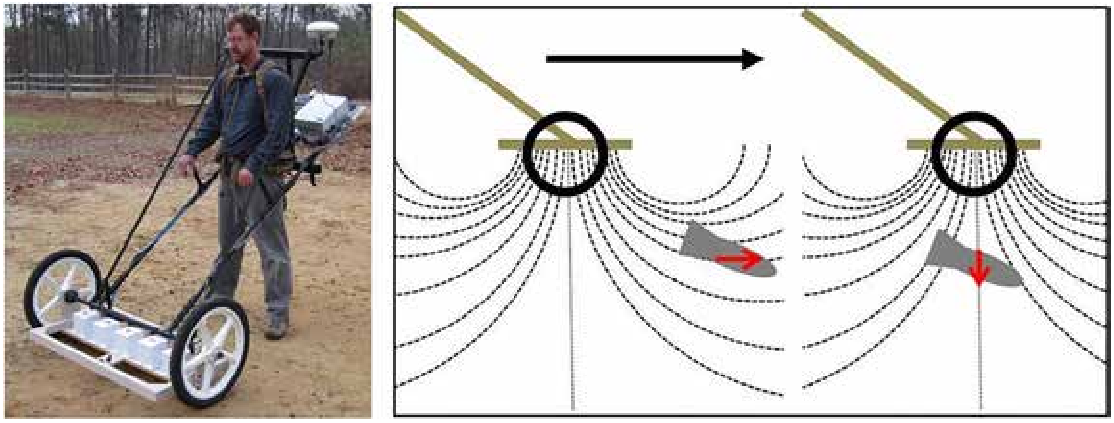

Figure 5: LEFT: The EMPACT man-portable array includes a single 1.0m wide by 0.5m long horizontal transmitter coil and 5 triaxial receivers. RIGHT: Because the sensor utilizes a single transmitter, effective classification is performed using a combination of multiple soundings along a transect line. As the array passes over the target, the change in the magnetic field (dashed lines) incident angle produces different angles of excitation within the target (indicated by red arrows).

For optimal classification results, we have found that it is best to include soundings from adjacent transect lines in the composite data set to ensure complete three-axis characterization of the target. Greater overlap in adjacent transects will produce higher quality classification; however, it is possible to achieve effective clutter rejection (discrimination) without overlap in sensor coverage. The line method uses point-to-point position and orientation tracking of the sensor as it acquires soundings along the transect line. Real Time Kinematic Differential GPS (RTK DGPS) or a linear positioning system (e.g., line encoder) providing 3-5 cm accuracy is sufficient for obtaining effective classification features. For operations in relatively flat terrain, orientation tracking of the array is not necessary; however, for sensor pitch and roll variations exceeding ~10 degrees, an inertial tracking unit can be used to monitor orientation changes. Figure 6 shows classification features and model parameters produced by inverting a composite set of soundings acquired along two adjacent DGM transect lines over an anomaly. An RTK DGPS provided the point-to-point position data for each sounding.

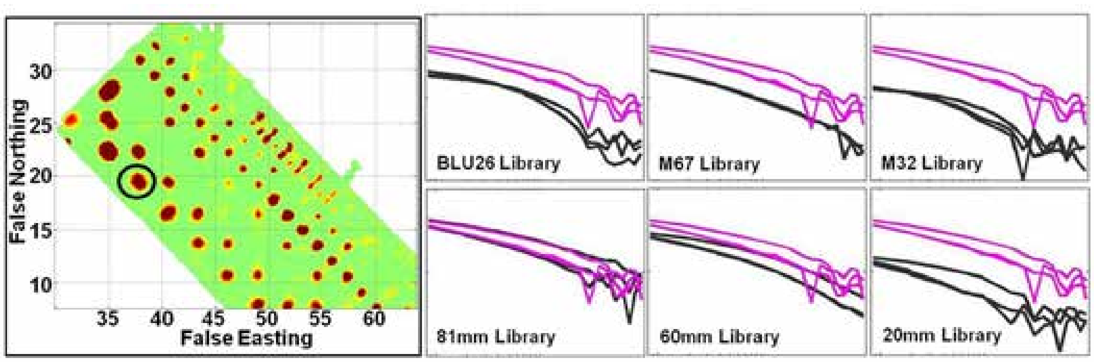

Figure 6: LEFT: EMPACT man-portable system DGM map (mV) showing the anomaly of interest circled in black. Soundings acquired along adjacent transect lines covering the anomaly are aggregated to form a composite data set for inversion. RIGHT: One set of polarizabilities (primary, secondary, and tertiary shown in magenta) are obtained from the inversion of the composite data. Polarizabilities are plotted as a function of time (logarithmically spaced) from 0.1 to 10 ms against library polarizabilities (dark grey curves) showing a match to the 81mm TOI. Polarizability units are arbitrary and correspond to the sensor output units.

Advanced DGM: Target Picking and Classification

We recently demonstrated both DGM systems at a Standardized UXO Technology Demonstration Site for performance assessments. We conducted mapping surveys with both systems operating in blind test field areas within the site (Figure 7). The objective of these demonstrations was to evaluate the ability of each system to enable both detection and classification of MEC items from data acquired during the mapping surveys. We treated each survey as a standard DGM operation, running both sensors along straight line transects across the survey area at approximately 2.5 km/h.

Figure 7: Vehicle-towed (LEFT) and man-portable (RIGHT) systems during DGM surveys at one of the DOD Standardized UXO Technology Demonstration Sites.

The initial post-survey analysis includes standard filtering and gridding of the survey data to produce two-dimensional maps corresponding to all survey areas. From these maps, we identify all anomalies exceeding our pre-determined threshold. These anomalies are then used as inputs to our inversion and classification software toolbox, which selects soundings for inversion and generates a set of classification features corresponding to individual regions of interest (ROI). The final step in the post-survey analysis processing chain is classification ranking (i.e., high probability UXO at the top of the list to high probability clutter at the bottom of the list) of each ROI. Initial ranking is based on an analysis of features such as size, decay, and symmetry and matching of polarizabilities to known UXO target polarizabilities. After initial ranking, the analyst performs a final quality control (QC) check of each ROI ranking.

During our QC analysis, the benefits of advanced DGM classification were exceedingly evident. The ability to correlate classification features with 2-D map features acquired from the same data set has a significant advantage over the two-step DGM + cued approach when analyzing data acquired in high anomaly density areas. This is exemplified in Figure 8 where data acquired over two targets produced overlapping anomalies in the 2-D detection map. Using a standard peak detection target picking algorithm, it is difficult to separate the anomaly into separate responses. In this case, if a cued sensor were to follow a standard DGM sensor, the target picking analysis might direct the cued sensor to a location between the two targets and fail to characterize them individually. Using the advanced DGM data, however, we can clearly separate soundings associated with one object from soundings associated with the adjacent object during the classification analysis. In this case, one group of soundings clearly indicates a TOI (81mm) while the other group of soundings indicates a large piece of clutter. Because both objects are of comparable size and emplaced at similar depths in close proximity, it would be difficult to distinguish their locations for a follow-up cued survey using the standard DGM approach.

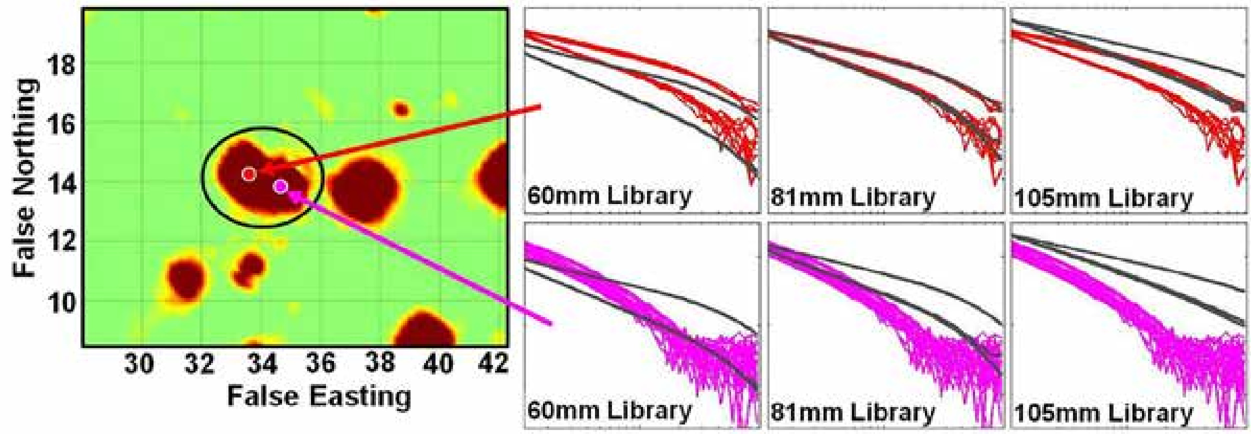

Figure 8: LEFT: OPTEMA DGM data map (nanoTesla/sec) showing the anomaly of interest circled in black. Using the 2-D data, it is difficult to resolve the location of the sources; however, classification analysis of the data reveals two distinct sources. RIGHT: Polarizabilities in arbitrary units (red and magenta curves) generated from classification analysis of the data plotted as a function of time (logarithmically spaced) from 0.1 to 8 ms against library polarizabilities (dark grey curves). Soundings from within the ROI (circled in black) are inverted for classification features. One set of soundings clearly indicates the presence of an 81mm TOI (red polarizability curves corresponding to a source location indicated by the red dot on the map) while another set of soundings indicates a large piece of clutter (magenta polarizability curves corresponding to a source location indicated by the magenta dot on the map).

The second example is presented in Figure 9, which shows data acquired over an area containing a bunch of clutter items. In this case, the peak detector identifies eight potential target sources. If a follow-up cued sensor were used here, the cued sensor would need to be moved around to eight different locations, requiring several minutes to complete. Using the advanced DGM data for classification, however, it is apparent that there are only three significant sources in the area, all of them similar clutter objects.

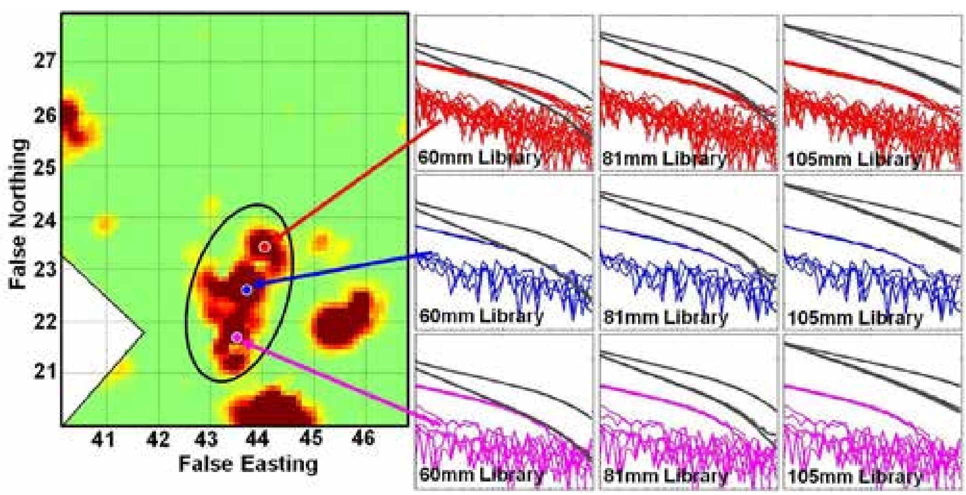

Figure 9: LEFT: OPTEMA DGM map showing the ROI circled in black (nanoTesla/sec). This ROI corresponds to a cluster of targets. Using the threshold target picking algorithm, the peak detector generates eight potential source locations in the ROI. If a follow-up cued survey were used, it would entail soundings at each of these eight locations, requiring several minutes to complete. RIGHT: Polarizabilities (red, blue, and magenta curves) generated from classification analysis of the data plotted as a function of time (logarithmically spaced) from 0.1 to 8 ms against library polarizabilities (dark grey curves). The polarizabilities in arbitrary units are divided into three groups (red, blue, magenta), each group corresponding to the location of a distinct clutter object in the DGM map (red, blue, magenta dots).

System Performance Summary and Conclusions

Results from recent performance evaluations show the ability of advanced DGM methods to enable a high degree of clutter rejection from mapping survey data. The vehicle-towed system enabled rejection of 85% of the clutter with 100% detection rate. This clutter rejection rate is comparable to those provided by advanced cued systems (McClung and others, 2009a; McClung and others, 2008; McClung and others, 2011) while the detection capabilities exceed those of standard DGM arrays (McClung and others, 2009b). This combination of high quality detection and discrimination from an advanced DGM survey makes it possible to greatly improve the productivity of the existing two-step detection/cued classification approach while retaining the same level of clutter rejection (typically >75%).

Analysis of data collected at the DOD UXO Demonstration Site emphasizes the significance of performing target picking and classification steps using one data set. By providing high resolution mapping data, the advanced DGM approach enables direct correlation of classification features to a set of 2-D map coordinates. This capability greatly improves the confidence of classification decisions made in high anomaly/clutter density areas by providing the analyst with a complete understanding of the target space.

Our recent tests indicate that advanced DGM classification is an efficient and reliable solution for munitions response site projects. Combining the anomaly detection, clutter rejection, and UXO/MEC classification stages in one DGM survey offers significant improvements to the two-step detection/classification approach currently used for many classification-level projects. These improvements are realized through a reduction in the number of excavations required for non-hazardous objects, a reduction in the total survey time required for detection and classification of all MEC contaminants, and greater reliability of the QC process due to the use of a single sensor for detection and classification.

Acknowledgments

The authors would like to acknowledge the Environmental Security Technology Certification Program and the U.S. Army for supporting development and testing of the aforementioned advanced DGM sensor technologies. We would also like to thank Daniel Steinhurst, David George, and Stephen Billings for support during preliminary testing and evaluation of the OPTEMA system components.

References

Andrews, A., and Nelson, H., 2011, Implementing advanced classification on munitions response sites: a guide to informed decision making for project managers, regulators, and contractors: Environmental Security Technology Certification Program (ESTCP) final report.

Andrews, A., Nelson, H., and Kaye, K., 2011, Classification approaches in munitions response, Camp Butner, North Carolina: Environmental Security Technology Certification Program (ESTCP) pilot program final report.

Bell, T., Barrow, B., Miller, J., and Keiswetter, D., 2001, Time and frequency domain electromagnetic induction signatures of unexploded ordnance: Subsurface sensing technologies and applications, vol. 2, no. 3, p. 153 – 175.

McClung, J.S., Teefy, D., Burch, W., Fling, R., and McClung, C., 2008, Standardized UXO technology demonstration site scoring record NO. 920: U.S. Army Aberdeen Test Center report.

McClung, J.S., Teefy, D., Burch, W., Fling, R., and McClung, C., 2009a, Standardized UXO technology demonstration site scoring record NO. 921: U.S. Army Aberdeen Test Center report.

McClung, J.S., Teefy, D., Burch, W., Fling, R., and McClung, C., 2009b, Standardized UXO technology demonstration site scoring record NO. 923: U.S. Army Aberdeen Test Center report.

McClung, J.S., Lombardo, L., Burch, W., Fling, R., and McClung, C., 2011, Standardized UXO technology demonstration site scoring record NO. 933: U.S. Army Aberdeen Test Center Report.

Miller, J.S., Zelt, B., and Lutes, D., 2013, In-field quality control of advanced electromagnetic induction data for munitions remediation projects: Proceedings of SPIE detection and sensing of mines, explosive objects, and obscured targets XVIII, v. 8709, p. 87090A-1 – A-10.

Shubitidze, F., O'Neill, K., Barrowes, B.E., Shamatava, I., Fernandez, J.P., Sun, K., and Paulsen, K.D., 2005, Application of the normalized surface magnetic charge model to UXO discrimination in cases with overlapping signals: Journal of Applied geophysics, v. 61, p. 292 – 303.

FastTIMES

UXO Geophysics:

Detection and Mapping of UXOs by Electromagnetic Induction Sensor and Self-Tracking Total Station

Case Study: Classification of MEC Targets Using Advanced TDEM Instruments and Analysis

A Man Portable EMI System for Detection and Classification of Unexploded Ordnance in Challenging Environments

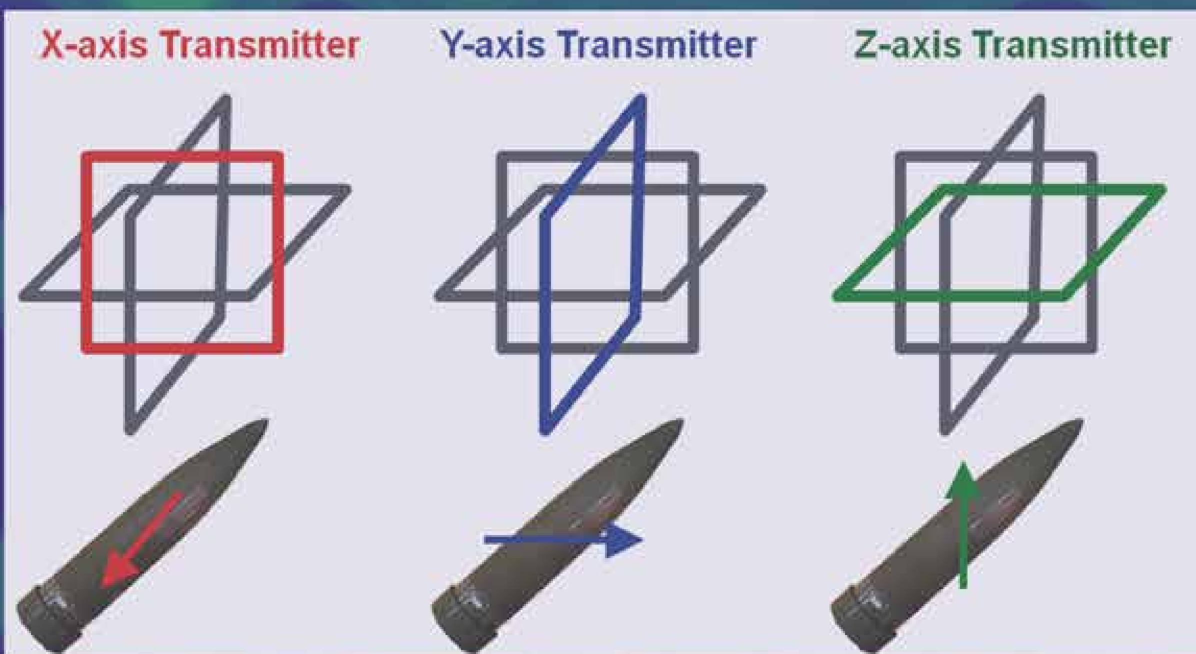

Dynamic UXO Classification Sensors: Advanced Digital Geophysical Mapping for Munitions Response Sites

Higher-Resolution Mapping for UXO Including Detection of 20mm Projectiles at Depth

Advanced Classification: What We've Learned and Where We're Heading

September 2014
Volume 19, Number 3